

**A sodium-mediated structural switch that controls the sensitivity of Kir channels to  
PIP<sub>2</sub>.**

Avia Rosenhouse-Dantsker<sup>1</sup>, Jin L. Sui<sup>2</sup>, Qi Zhao, Radda Rusinova,  
Aldo A. Rodríguez-Menchaca<sup>3</sup>, Zhe Zhang<sup>3</sup>, and Diomedes E. Logothetis<sup>3,\*</sup>

*Department of Structural and Chemical Biology, Mount Sinai School of Medicine, New  
York, New York 10029*

**1 Current address:** Department of Medicine, Section of Pulmonary, Critical Care and Sleep Medicine, University of Illinois at Chicago, 840 South Wood Street (M/C 719), Room 920-N CSB, Chicago, IL 60612

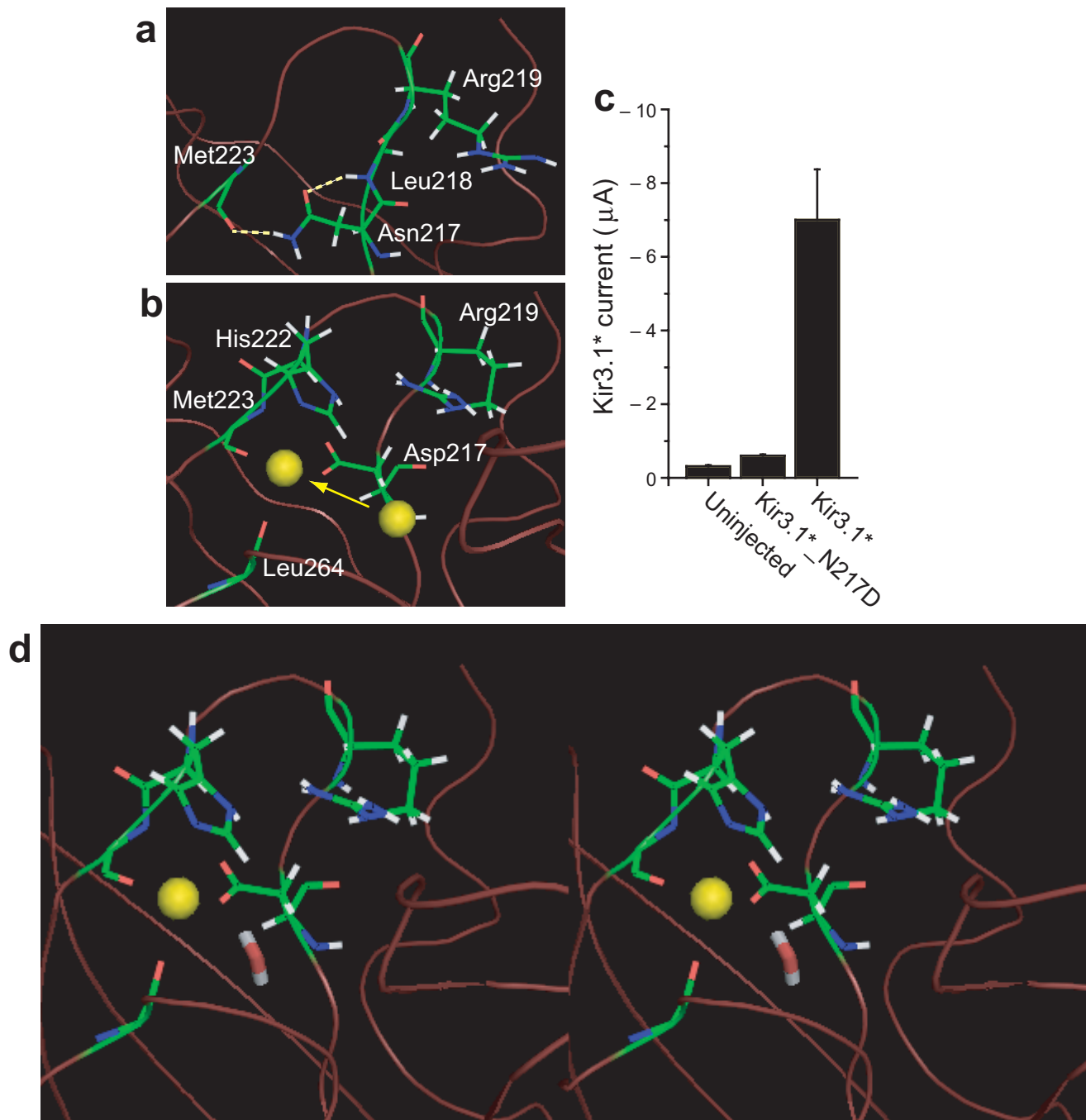
**2 Current address:** CombinatoRx Inc., 245 First Street, Cambridge, MA 02142

**3 Current address:** Virginia Commonwealth University, Medical College of Virginia Campus, Department of Physiology and Biophysics, Sanger Hall 3-005, 1101 E. Marshall Street, Richmond, VA 23298

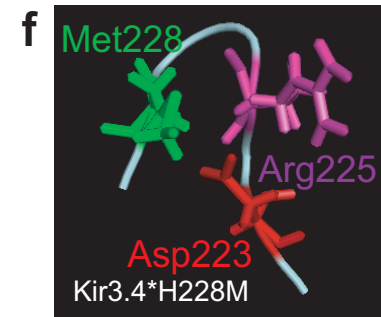
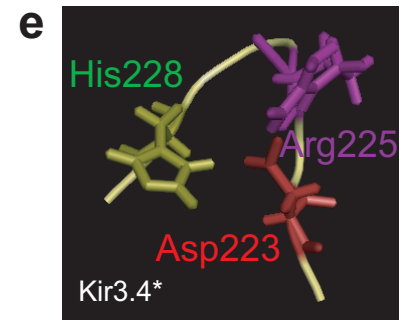
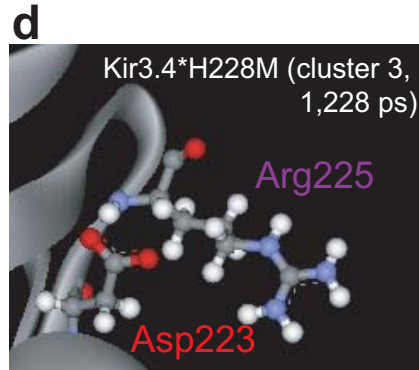
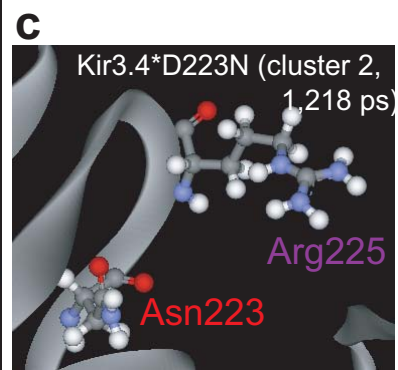
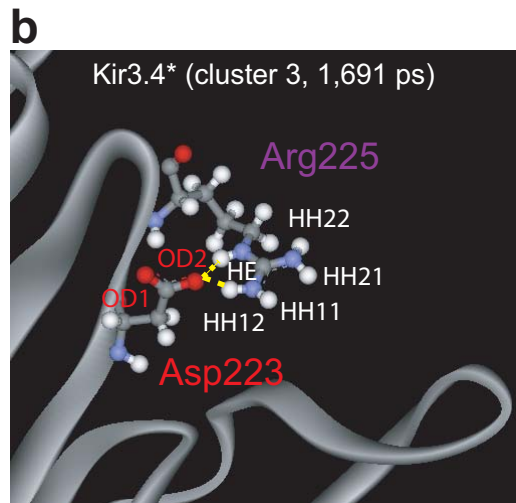
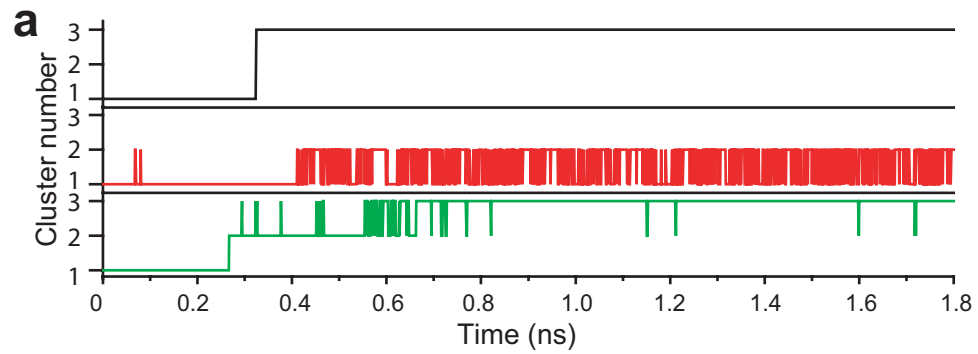
\* To whom correspondence should be addressed: delogothetis@vcu.edu

**Running title:**

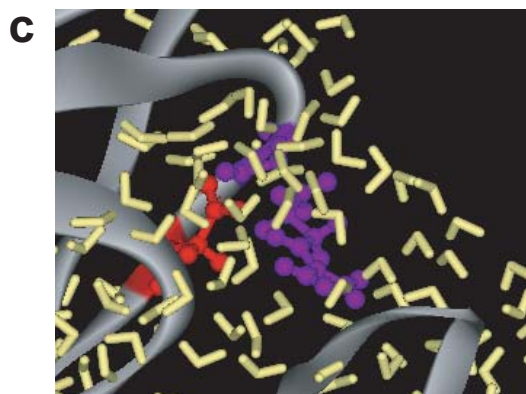
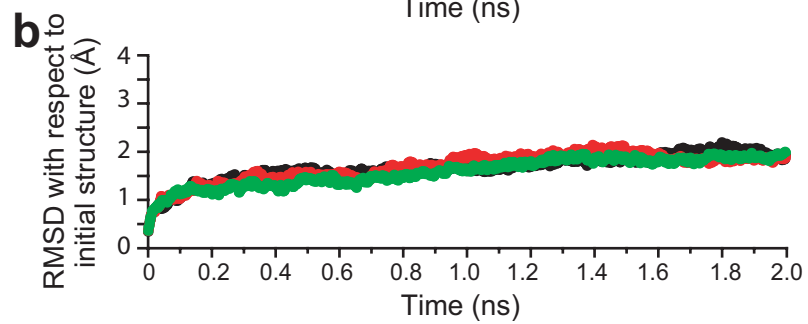
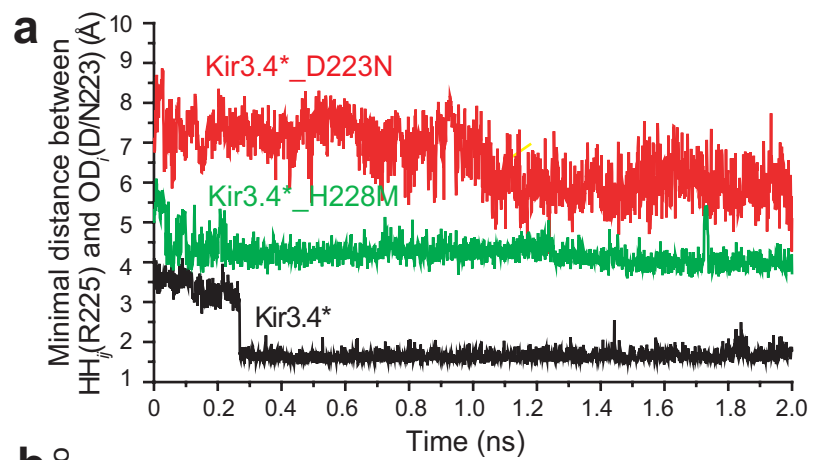
**Sodium mediated structural switch**



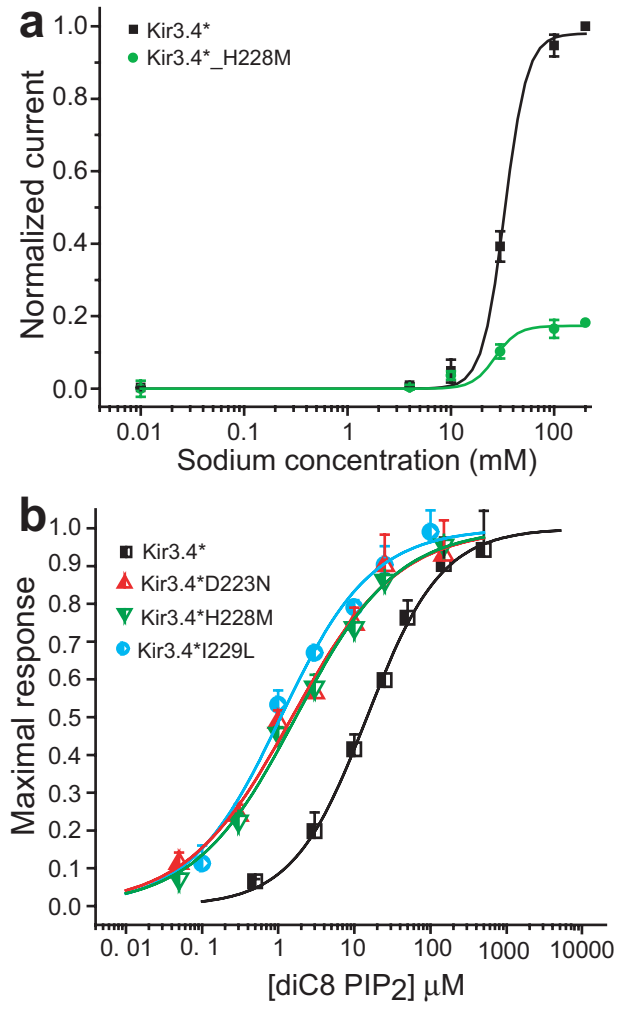
**Supplemental Figure 1.** H-bonding pattern between position 217 and residues in its vicinity in **(a)** Kir3.1 after minimization. The model was based on the crystallographic structure of Kir3.1 (PDB accession number 1N9P<sup>19</sup>). **(b)** 4.6Å displacement of a Na<sup>+</sup> ion during minimization to its coordination site. **(c)** Summary of whole-cell basal current from Kir3.1\* and Kir3.4\*\_N217D expressed in *Xenopus* oocytes and recorded at -80mV. **(d)** Stereo view of the sodium coordination site in Kir3.1\_N217D that shows a nearby water molecule. Figures **(a)**, **(b)**, and **(d)** were drawn using PyMol<sup>48</sup>.



**Supplemental Figure 2.** Conformational transitions revealed through clustering analysis. **(a)** Classification of the structures obtained during the MD simulations of Kir3.4, Kir3.4\_D223N, and Kir3.4\_H228M according to clustering analysis. **(b)-(d)** Representative conformations of the backbone atoms of the critical loop of dominant clusters obtained from the simulation of Kir3.4, Kir3.4\_D223N and Kir3.4\_H228M portraying the relative orientations of the side-chains of positions 223 and 225. **(e)-(f)** Orientations of the side-chains of position 223, 225 and 228 in the representative conformations of the dominant clusters of Kir3.4 and in Kir3.4\_H228M.

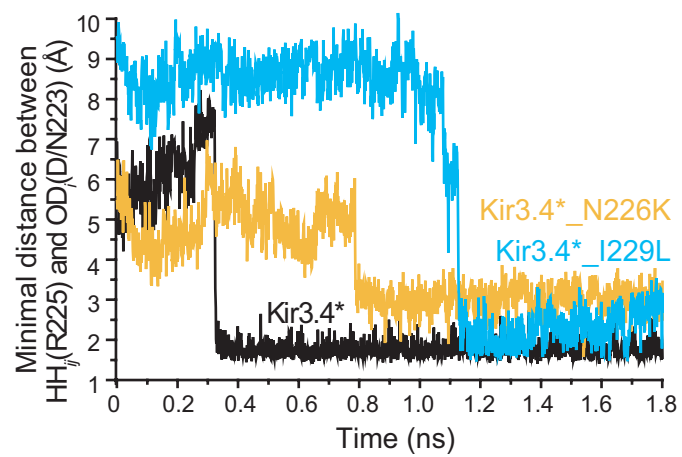


**Supplemental Figure 3.** Simulations in the presence of water. **(a)** Minimal distance between positions 223 and 225 as obtained from MD simulations of Kir3.4\*, Kir3.4\*\_D223N, and Kir3.4\*\_H228M in the presence of the primary hydration shell (PHS - see methods). **(b)** RMSD of the backbone residues of the cytosolic domain relative to the starting minimized structure that corresponds to the MD simulations of Kir3.4, Kir3.4\_D223N, and Kir3.4\_H228M in the presence of the PHS. The calculations were performed using Simulaid: <http://atlas.physbio.mssm.edu/~mezei/simulaid/simulaid.html>. **(c)** Representative structure of the critical loop in Kir3.4 surrounded by the PHS.

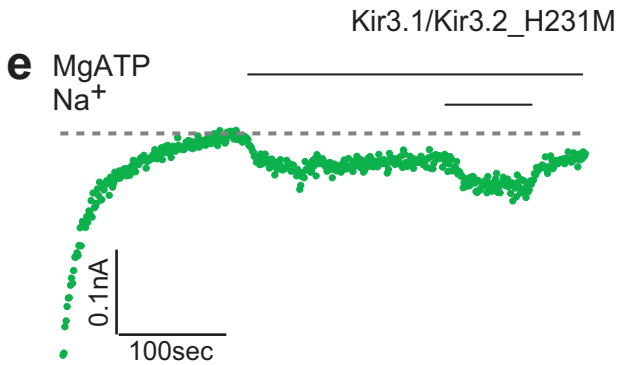
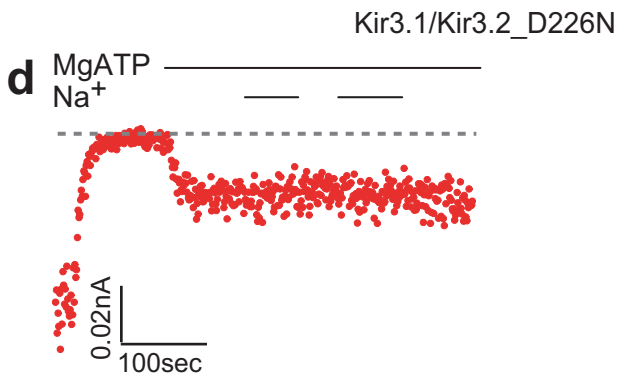
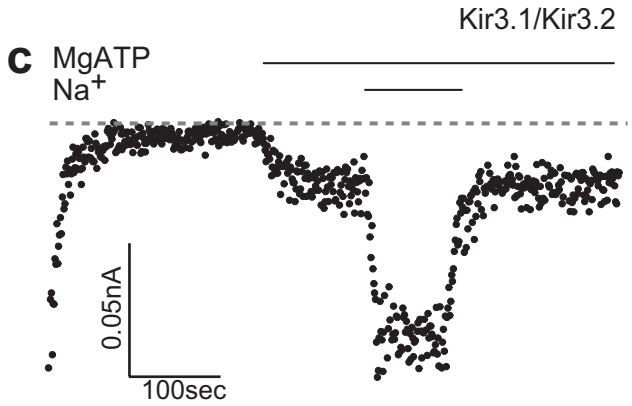
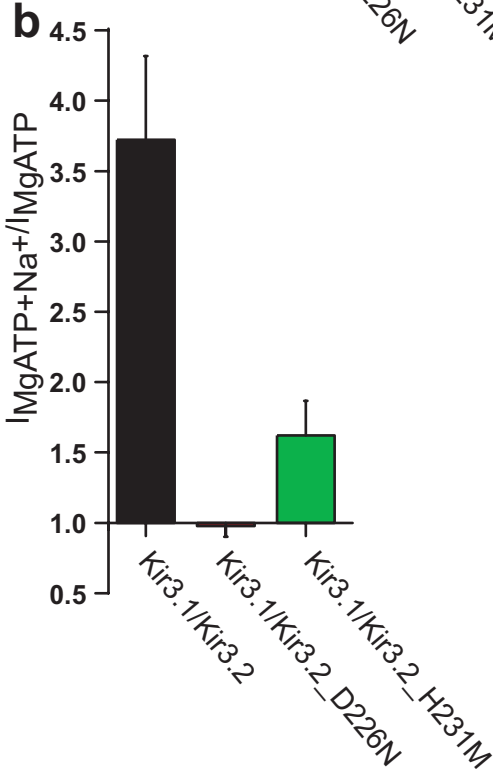
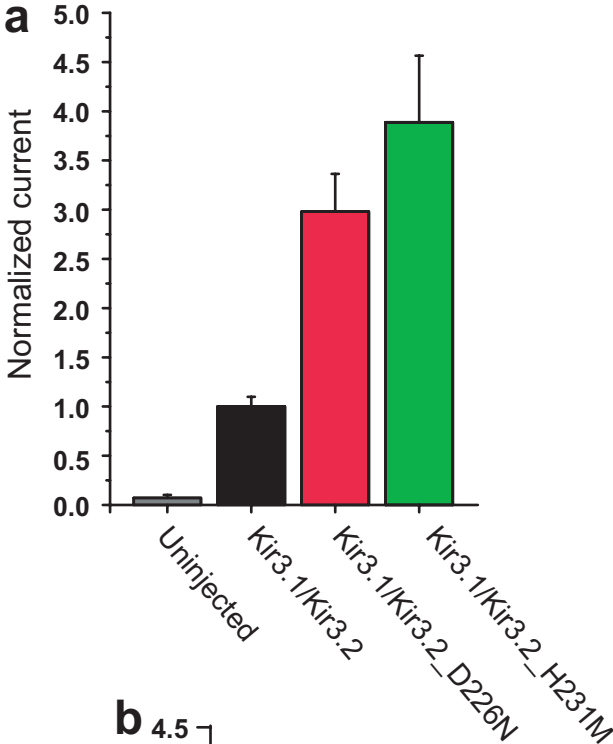




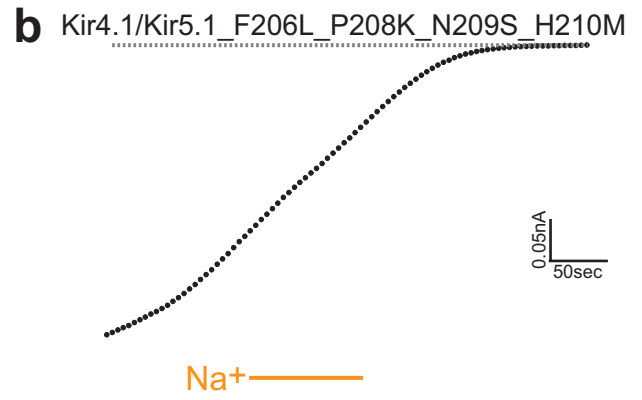
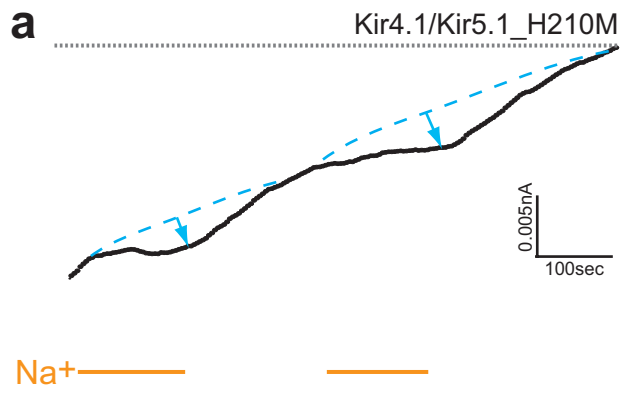
**Supplemental Figure 4.** Effects of mutations of Kir3.4\* residues in the loop where Na<sup>+</sup> is coordinated on Na<sup>+</sup> and PIP<sub>2</sub> sensitivity **(a)** Na<sup>+</sup> dose-response curve of Kir3.4\* and Kir3.4\*\_H228M obtained in the presence of 3μM PIP<sub>2</sub>. **(b)** PIP<sub>2</sub> dose-response curves of Kir3.4\*, Kir3.4\*\_D223N, Kir3.4\*\_H228M, and Kir3.4\*\_I229L obtained using diC8 in the presence of 30mM Na<sup>+</sup>.



**Supplemental Figure 5.** MD simulations monitoring distance of Na<sup>+</sup>-insensitive neighboring residues to Kir3.4\*\_R225. Minimal distance between positions 223 and 225 as obtained from MD simulations of Kir3.4, Kir3.4\_N226K, and Kir3.4\_I229L.



**Supplemental Figure 6.** Experimental evidence for Kir3.2 residues involved in Na<sup>+</sup> sensitivity **(a)** Whole-cell basal currents of Kir3.1/Kir3.2, Kir3.1/Kir3.2\_D226N, and Kir3.1/Kir3.2\_H231M recorded in *Xenopus* oocytes at -80mV. **(b)-(d)** Representative traces of inside-out macropatch recordings of *Xenopus* oocytes. Na<sup>+</sup> (30mM) and MgATP (5mM) were applied as indicated by the bars in the control solution (ND96K+EGTA with 2mM Mg<sup>++</sup>) **(b)** Kir3.1/Kir3.2 **(c)** Kir3.1/Kir3.2\_D226N **(d)** Kir3.1/Kir3.2\_H231M. **(e)** Summary data showing the effect of perfusion of Na<sup>+</sup> (30mM) on currents obtained from inside-out patches of *Xenopus* oocytes after a short application of MgATP (5mM).



**Supplemental Figure 7.** Experimental evidence of a role for His210 in Na<sup>+</sup> sensitivity of Kir5.1. **(a)** The rundown of Kir4.1/Kir5.1\_H210M is still slowed down following application of sodium. **(b)** The rundown of Kir4.1/Kir5.1\_F206L\_P208K\_N209S\_H210M becomes Na<sup>+</sup> insensitive.

Supplemental Table 1: Summary of the cluster analysis of the trajectories obtained from the molecular dynamics simulations of Kir3.4, Kir3.4\_D223N, and Kir3.4\_H228M according to the distances between the atoms in the side-chains of the residues at positions 223 and 225 that could form hydrogen bonding.

Cluster number	number of members	Average distance (Å)									
		OD1(223)-HH11(225)	OD1(223)-HH12(225)	OD1(223)-HH21(225)	OD1(223)-HH22(225)	OD1(223)-HE(225)	OD2(223)-HH11(225)	OD2(223)-HH12(225)	OD2(223)-HH21(225)	OD2(223)-HH22(225)	OD2(223)-HE(225)
Kir3.4											
1	323	8.138	7.454	7.502	6.286	5.675	9.858	9.163	9.14	7.843	7.31
2	1	8.22	6.856	8.581	7.972	5.18	6.236	4.748	7.02	6.75	3.544
3	1476	5.466	3.74	7.006	7.034	3.666	3.574	1.78	4.934	4.958	1.688
Kir3.4_N216D											
1	991	8.186	6.663	9.757	9.699	6.548					
2	809	8.988	7.409	10.595	10.502	7.206					
Kir3.4_H228M											
1	266	8.729	8.033	7.991	6.704	6.125	10.722	10.097	9.816	8.46	8.18
2	342	10.671	10.153	9.585	7.963	8.106	8.834	8.328	7.786	6.17	6.297
3	1192	9.262	8.926	8.033	6.373	7.01	7.175	6.931	5.964	4.349	5.182